Microsyst Technol (2006) 12: 803–813
DOI 10.1007/s00542-006-0207-y

TECHNICAL PAPER

M. Rotunno · R. Oboe · R. A. de Callafon

Modeling product variations in hard disk drive micro-actuator suspensions

Received: 16 July 2004 / Accepted: 17 February 2006 / Published online: 30 May 2006

Abstract The increase in aerial storage capacities of future magnetic hard disk drives has fostered the use of dual-stage actuators for high track density data recording. In a hard disk drive with a dual-stage actuator the standard rotary actuation of the voice coil motor is combined with an additional micro or milli actuation to accomplish high-bandwidth and highly accurate track following. In order to guarantee error less data transfer, the track following servo controller needs to perform robustly under different operating conditions, that include changes in flying height and product manufacturing tolerance of the dual-stage actuator. Essential in the controller design is to characterize these uncertain conditions and design a robust track following servo accordingly. In this paper we present an experiment based methodology to characterize the varying servo conditions in the form of an uncertainty model. The uncertainty model can be used for analysis and synthesis of robust servo controllers.

1 Introduction

Significant progress in areal storage density of a magnetic hard disk drive (HDD) can be accomplished by using a dual-stage actuator system, in which a high-bandwidth and highly accurate micro-actuator (MA) is used in combination with a traditional voice coil motor (VCM) to position the read/write head on the slider over the data track (Fan et al. 1995; Li and Horowitz 2002; Li et al. 2003; Teerjuis et al. 2003). While most high density demonstrations are achieved under a well conditioned laboratory environment, HDD's incorporating dual-stage actuators will be subjected to all the variabilities that come with manufacturing and changing of operating conditions. If the same areal densities are to be achieved in low cost consumer applications, then the track following servo control system will need to be able to perform adequately in the presence of all possible product variabilities and uncertainties.

In modern control design approaches for dual-stage HDDs which make use of H_∞ and μ synthesis (de Callafon et al. 1999; Hernandez et al. 1999; Rotunno and de Callafon 2000) it is possible to incorporate the effects of product variations and various operating conditions in the design process in the form of an uncertainty model. The uncertainty model consists of a nominal model together with a description of the perturbation of the nominal model. The first step in obtaining a servo control system that is robust with respect to product variability, consists of characterizing the variations and uncertainties of the micro-actuator system.

This paper focuses on product variabilities that arise from variations in Z-height and variations from one suspension to another due to manufacturing. These variations and uncertainties will have a strong effect on the effectiveness of a high-bandwidth and highly accurate dual-stage servo controller design. Experimental data and a systematic modeling and uncertainty characterization are used to capture the variabilities of a dual stage actuator. The methodology is tested out on a dual-stage actuator produced by Hutchinson Technology Inc. (HTI). Once an uncertainty model has been characterized, a robust servo controller can be synthesized using an H_∞ based control methodology.

M. Rotunno
Research and Development Aerostudi, SpA viale del Lido 37, Rome 00122, Italy

R. Oboe
Department of Electronics and Informatics, University of Padova, via Gradenigo 6/a, 35131 Padova, Italy

R. A. de Callafon (✉)
Department of Mechanical and Aerospace Engineering, University of California, 9500 Gilman Drive, La Jolla, San Diego, CA 92093-0411, USA
E-mail: callafon@ucsd.edu
Tel.: +1-858-3444265
Fax: +1-858-8223107

2 Product variability

2.1 PZT micro-actuator suspension

The experimental results produced in this paper are based on a piezoelectric dual-stage suspension manufactured by Hutchinson and a picture of the dual-stage actuator is shown in Fig. 1. In this HTI Magnum 5E piezoelectric dual-stage suspension, two PZT bars are used to move the slider in a direction perpendicular to the track by a push–pull configuration. In a hard disk with multiple disks, several dual-stage suspension are mounted on a single E-block. The E-block connects the suspensions to a radial VCM for the gross movements of the read/write head. The piezo-electric dual-stage actuator can be used as a secondary actuator for the fine movements of the read/write head.

Experiments were conducted to observe the variations in the dynamic behavior of the dual-stage suspension. The variations are primarily caused by production and manufacture variations for different suspensions. Additionally, variations in the dynamic behavior were observed due to changes in the Z-height, which is the distance from the E-block connection to the hard disk. Variations in the Z-height change the flying height and the air-bearing stiffness of the slider, resulting in different dynamical aspect of the micro-actuator. Both conditions reflect the effects of manufacturing tolerances and changing flying height conditions for a set of dual-stage suspension mounted on a single E-block. As multiple suspension are controlled by a single servo controller, these variations have to be taken into account when designing a robust dual-stage servo controller for track following.

2.2 Experimental data

The variations in the dynamical behavior of the dual-stage suspension is examined by measuring frequency response functions (FRF) of the suspensions. For that purpose a Spin Stand with a 7,200 rpm drive, a Polytech Laser Doppler Velocimeter (LDV) position measurement system and a DSP Siglab data analysis system are used. The DSP board generates a random signal of prescribed intensity which is amplified to the desired voltage level by a ST Micro piezo driver and applied to the piezo pads on the suspension. The slider position is measured by the LDV and fed back to the DSP board where a transfer function estimate is computed.

For notation purposes, let $u(t)$, $t = 1,...,N$ indicate the discrete signal generated by the DSP board and $y(t)$ the slider position measured by the LDV. Then the discrete Fourier transforms of $u(t)$ and $y(t)$ are given by:

$$U_N(\omega) = \frac{1}{\sqrt{N}} \sum_{t=1}^{N} u(t) \exp^{-i\omega t} \tag{1}$$

$$Y_N(\omega) = \frac{1}{\sqrt{N}} \sum_{t=1}^{N} y(t) \exp^{-i\omega t} \tag{2}$$

the empirical transfer function estimate (ETFE) is given by Ljung (1999)

$$\hat{F}(\omega) = \frac{Y_N(\omega)}{U_N(\omega)} \tag{3}$$

To reduce the effects of measurement noise and the variance of the ETFE, the estimate given in Eq. 3 is averaged over several measurements. This greatly improves the variance aspects of the ETFE, leading to unbiased and consistent estimate of the FRF of the dual-stage actuator.

To indicate the quality of the FRF measurements, a typical frequency response of an HTI suspension is shown in Fig. 2. For illustration purposes, only the amplitude Bode response of the FRF measurement is shown in Fig. 2. It can be observed from this figure that the dual-stage actuator exhibits a dynamical behavior

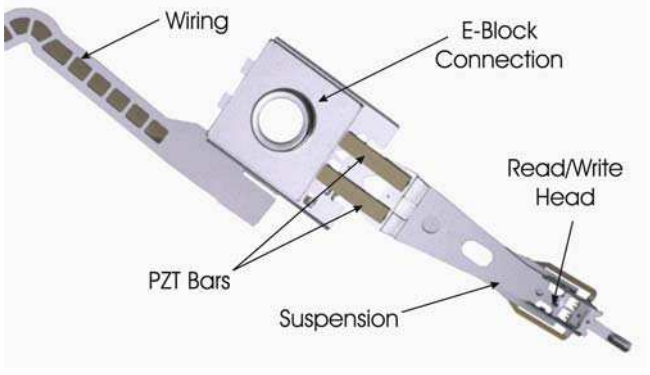

Fig. 1 HTI Magnum 5E piezoelectric dual-stage suspension

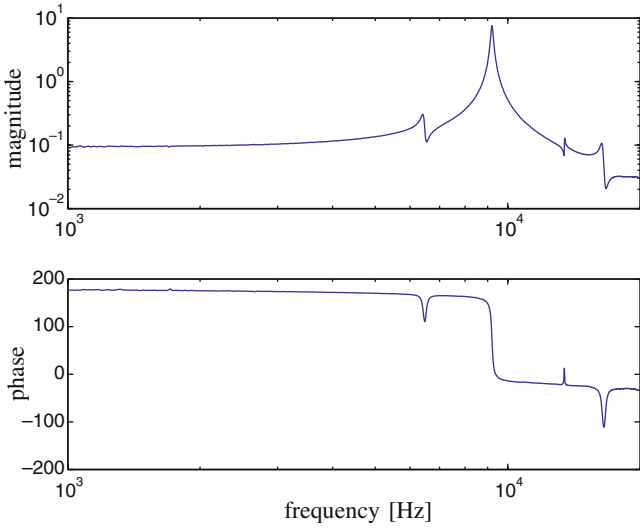

Fig. 2 Typical amplitude (*top*) and phase (*bottom*) Bode frequency response function of an HTI dual-stage suspension

that involves a major resonance mode at 9 kHz, which corresponds to the first sway mode of the suspension. Additional small resonance and anti-resonance modes are observed around 6.5 and 13 kHz that can be contributed to torsional modes of the suspension. Variations in both manufacturing and in mounting conditions, such as the distance in spacing between suspension mounting and the hard disk (Z-height), will modify the location and height of these resonance modes in the frequency domain measurements. As an example it is worth mentioning here that variations in the Z-height has a significant effect on the torsion modes fop the suspension. These variations are illustrated in the following.

2.3 Manufacturing variations

With a fixed Z-height, it is possible to compare the frequency response data of various suspensions for manufacturing variabilities. At a fixed Z-height of 22 micro inches or 0.56 mm, in Fig. 3 FRF measurements $F_k(\omega)$, $k=1,...,7$ of seven different dual-stage suspensions are compared. It can be noted that there can be substantial difference between the frequency response of the various suspensions, especially at the first torsion mode around 6.5 kHz.

The variations in the dynamic behavior of the dual-stage suspension due to manufacturing variations or production tolerances play an important role in the design of high performance (high bandwidth) dual-stage servo controllers. Only one single servo controller will be used to control several dual-stage suspensions in a single HDD. As a result, the dual-stage servo should be designed such that it is robust against the variations in the dynamic behavior to avoid servo performance deterioration.

2.4 Variations in Z-height

The dual-stage suspensions were also tested for Z-height variations: the distance from the E-block connection to the magnetic recording surface of the hard disk. Variations in the Z-height will alter the flying height and air bearing properties of the slider on which the read/write head is mounted. For experimental purposes, the Z-height is varied 10 milli inches or 0.26 mm around the nominal value of 0.56 mm to simulate excessive Z-height variations in a HDD. It should be noted that such variations are much larger than typically observed in a suspension mounted in a HDD the results are solely used to demonstrate the effectiveness of capturing possible structural variations in the torsion mode of the suspension. Measured frequency response functions $F_k(\omega)$ of one dual-stage suspension for which the Z-height is varied between 0.30 mm and 0.82 mm is depicted in Fig. 4.

It is observed from the data in Fig. 4 that the smallest value of the Z-height (0.30 mm), significantly decreases the torsion mode at approximately 6.5 kHz. The largest value of the Z-height (0.82 mm) causes a significantly large torsion mode. Henceforth, the FRF measurements due to variations in Z-height from 0.30 to 0.82 mm in Fig. 4 can be distinguished by the size of the torsion mode around 6.5 kHz. The effect of Z-height is clearly demonstrating the changing boundary conditions of the air bearing, causing the dual-stage suspension to act more as cantilevered beam with a less restricted torsion mode.

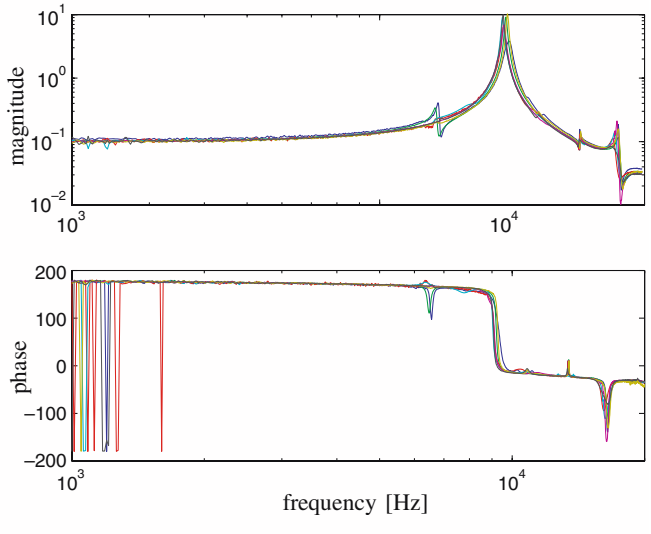

Fig. 3 Magnitude (*top*) and phase (*bottom*) Bode plot of the frequency response for seven different dual-stage suspensions all mounted and flying over an 7,200 RPM operating hard disk at a Z-height of 22 milli inches or 0.56 mm

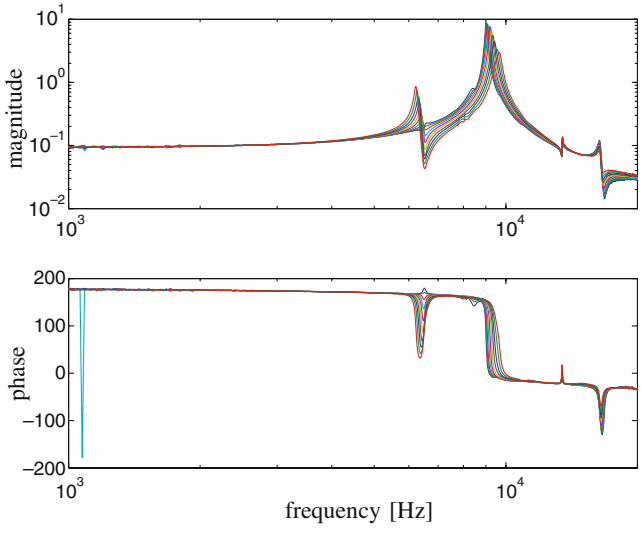

Fig. 4 Magnitude (*top*) and phase (*bottom*) Bode plot of the frequency response of a single dual-stage suspension for Z-height variations between 0.30 and 0.82 mm

3 Uncertainty modeling

3.1 Uncertainty models

From the experimental results it can be observed that a single linear dynamical model P will not capture the dynamical variations in the dual-stage suspension. Instead of formulating a single dynamical model, a set of models $\mathscr{P}$ can be proposed to account for the variations in the FRF measurements of the dual-stage actuators. The set of models $\mathscr{P}$ needs to be constructed in such a way, that all measured FRF can be represented in the set $\mathscr{P}$. In case this set of models $\mathscr{P}$ is constructed in conformance with robust control design techniques, a robust dual-stage servo controller can be designed and analyzed to account for the variations in the dynamical behavior in the dual-stage suspensions.

A set of models $\mathscr{P}$ that is conform with robust servo control design techniques is described by norm bounded perturbation in a linear fraction transformation (LFT) framework. Such a set of models $\mathscr{P}$ is described by

$$\mathscr{P} = \{P | P = \mathscr{F}_u(Q, \Delta), \|\Delta\|_\infty \leq 1\} \tag{4}$$

where Δ indicates a stable norm bounded perturbation and

$$\mathscr{F}_u(Q, \Delta) = Q_{22} + Q_{21}\Delta(I - Q_{11})^{-1}Q_{12} \tag{5}$$

denotes the upper linear fractional transformation (LFT) of Δ with the four transfer functions in the transfer function matrix

$$Q = \begin{bmatrix} Q_{11} & Q_{12} \\ Q_{21} & Q_{22} \end{bmatrix}$$

In Eq. 5 Q_{22} is used describe the nominal dynamical behavior ($\Delta = 0$). The stable (and possibly structured) norm bounded perturbation Δ is the (allowable) perturbation, which encompasses the variability and uncertainty that arise due to changing of operating conditions or manufacturing tolerance. In general, the terms Q_{12}, Q_{21} and Q_{11} are additional dynamic models that specify and normalize the shape and location of the perturbation that occur in the nominal behavior Q_{22}.

The format of Q in Eq. 5 completely determines the uncertainty model and the corresponding set of models $\mathscr{P}$ in Eq. 4. The uncertainty model Q can be found by considering unstructured uncertainty perturbations in order to characterize variations with an unknown structure such as the effects of manufacturing variations for dual-stage actuators as illustrated in Sect. 2.3. Structured uncertainty perturbations can be used to model highly structured dynamical variations such as the possible changes in Z-height conditions discussed in Sect. 2.4. The distinction between unstructured uncertainty models for modeling product variabilities and structured uncertainty models for modeling Z-height conditions will be continued throughout the paper. More details can be found in the following sections.

3.2 Unstructured uncertainty description

In order to represent the various FRF $F_k(\omega)$ of the dual-stage actuators, an nominal model along with a uncertainty description is used. The effect of manufacturing variations for dual-stage actuators, that typically has an unknown structure, is chosen to be represented by a multiplicative uncertainty description

$$\mathscr{P}_\mathrm{m} = \{P | P = P_0(1 + W_\mathrm{m}\Delta_\mathrm{m}), \|\Delta_\mathrm{m}\|_\infty \leq 1\} \tag{6}$$

that is well suited for representing unstructured dynamical variations (Skogestad and Postlethwaite 1996; Zhou and Doyle 1998). In Eq. 6, P_0 is used to denote the nominal model and W_m is a weighting function which models the size and shape of the multiplicative perturbation. The frequency dependency of both the nominal model P_0 and the multiplicative uncertainty weighting function W_m will be indicated by the argument (ω) and both $P_0(\omega)$ and $W_\mathrm{m}(\omega)$ can be continuous or discrete time models.

The multiplicative uncertainty set in Eq. 6 is a special case of the LFT based uncertainty set in Eq. 4 with $Q_{11} = 0$, $Q_{12} = W_\mathrm{m}\, P_0$, $Q_{21} = 1$ and $Q_{22} = P_0$. Henceforth, to complete the multiplicative unstructured uncertainty description, both the nominal model P_0 and the weighting function W_m in Eq. 6 need to be modeled. In the next section it is shown how the nominal model P_0 and the multiplicative uncertainty weighting function can be estimated from the measured frequency response measurements $F_k(\omega)$ presented in Fig. 3. First, the structured uncertainty associated to Z-height variations is discussed.

3.3 Structured uncertainty description

As indicated in Sect. 2.4, Z-height variations typically cause a slight change in frequency and damping of the resonance (torsion) mode of the dual-stage suspension. Such variations can be captured very well in a structured uncertainty description with perturbations on stiffness and damping parameters of a model.

The discrete time nature of the servo controller in a HDD motivates the use of discrete time models in this paper. To describe the structured uncertainty associated with Z-height variations, consider a discrete time model $P(z)$ described by

$$P(z) = \frac{b_2 z^2 + b_1 z + b_0}{a_2 z^2 + a_1 z + a_0}, \quad z = e^{j\Delta T\omega} \tag{7}$$

where ΔT reflects the sampling time of the discrete time model P. For the analysis purposes of this section, the model P in Eq. 7 is chosen as a second-order discrete

time model and is used to reflect a varying resonance and anti-resonance mode present in the nominal model P_0.

From the data in Fig. 4 it can be observed that variations in Z-height do not cause DC variations, but only changes in location and damping of the torsion resonance mode located around 6.5 kHz. This can be included in Eq. 7 by assuming no gain variations of the transfer function $P(z)$ and a simple variable transformation

$$K=\frac{b_2}{a_2},\ \bar{b}_1=\frac{b_1}{b_2}-\frac{a_1}{a_2},\ \bar{a}_1=\frac{a_1}{a_2},\ \bar{b}_0=\frac{b_0}{b_2}-\frac{a_0}{a_2},\ \bar{a}_0=\frac{a_0}{a_2} \quad (8)$$

rewrites Eq. 7 into a monic transfer function with constant gain K

$$\begin{aligned} P(z) &= K\frac{z^2+(\bar{b}_1+\bar{a}_1)z+(\bar{b}_0+\bar{a}_0)}{z^2+\bar{a}_1z+\bar{a}_0} \\ &= K\left(1+\frac{\bar{b}_1z+\bar{b}_0}{z^2+\bar{a}_1z+\bar{a}_0}\right). \end{aligned} \quad (9)$$

In Eq. 9, the parameters $\bar{b}_1$ and $\bar{b}_0$ are now used to indicate a difference in the numerator coefficients with respect to the denominator coefficients.

The model parametrization in Eq. 9 can be used to characterize structured uncertainty in damping and stiffness in the torsion resonance/anti-resonance mode of the dual-stage actuator due to Z-height variations. Moreover, the parametrization (Eq. 9) allows the structured uncertainty to be represented in a LFT format. This can be seen as follows.

The interval for each parameter $\bar{b}_i$, $\bar{a}_i$, $i=0,1$ in Eq. 9 can be considering as a (structured) additive perturbation. The parameter perturbations are described by

$$\begin{aligned} \bar{b}_i &= b_{0,i}+r_{b,i}\delta_{b,i} \quad |\delta_{b,i}|<1, \quad i=0,1 \\ \bar{a}_i &= a_{0,i}+r_{a,i}\delta_{a,i} \quad |\delta_{a,i}|<1, \quad i=0,1 \end{aligned} \quad (10)$$

and indicate absolute changes in the parameters. In Eq. 10, $b_{0,i}$, $a_{0,i}$ denote the nominal parameter values, where as $r_{b,i}$, $r_{a,i}$ respectively denote the absolute size of the perturbation of the parameters.

The parametrization given in Eq. 9 can be represented by the block diagram given in Fig. 5. As the perturbation of each parameter $\bar{b}_i$, $\bar{a}_i$ in Eq. 10 can be written as a LFT, the combination of all parameter perturbations can be written in a structured uncertainty model using a LFT representation

$$\mathscr{P}_z=\{P|P=\mathscr{F}(Q,\Delta_z),\ \Delta_z=\mathrm{diag}(\delta_{b,1},\delta_{b,0},\delta_{a,1},\delta_{a,0})\} \quad (11)$$

where $|\delta_{b,i}|<1$, $i=0,1$, $|\delta_{a,i}|<1$, $i=0,1$. The entries of Q in the LFT representation of Eq. 11 can readily be found with Fig. 5 and Eq. 10.

Both the uncertainty model $\mathscr{P}_m$ in Eq. 6 for manufacturing variations and the uncertainty model $\mathscr{P}_z$ in Eq. 11 for Z-height variations are represented by LFT's. Both uncertainty models can be combined to capture both the product and Z-height variations in a single LFT based uncertainty model $\mathscr{P}$ similarly to Eq. 5 where the uncertainty Δ has been normalized and structured in a diagonal form $\Delta=\mathrm{diag}\,(\delta_{b,1},\ \delta_{b,0},\ \delta_{a,1},\ \delta_{a,0},\ \Delta_{\mathrm{m}})$ where $|\delta_{b,i}|<1$, $i=0,1$, $|\delta_{a,i}|<1$, $i=0,1$ and $||\Delta_{\mathrm{m}}||_\infty<1$. In the following, the estimation of the nominal model P_0 along with the uncertainty bounds on the basis of FRF measurements is discussed in more detail.

4 Application of uncertainty modeling

4.1 Role of nominal model

The nominal model P_0 plays an important role in the characterization of an uncertainty model. In case of the unstructured multiplicative uncertainty model $\mathscr{P}_{\mathrm{m}}$ mentioned in Eq. 6, the choice of a nominal model P_0 directly affects the weighting function W_{m}. An appropriate choice of P_0 can lead to a small multiplicative uncertainty bound W_{m} which in turn is favorable for the design of a robust performing servo controller.

Given the FRF measurements $F_k(\omega)$ of several dual-stage actuators and a choice of for a single nominal model P_0, an upper bound for the unstructured multiplicative uncertainty can be computed by

$$\delta_m(\omega)=\max_k\left\|\frac{F_k(\omega)-P_0(\omega)}{P_0(\omega)}\right\|,\quad \omega\in\Omega \quad (12)$$

At a frequency point ω at the frequency grid Ω, the frequency dependent function $\delta_{\mathrm{m}}(\omega)$ is simply the worst case upper bound between the nominal model $P_0(\omega)$ and each frequency response function $F_k(\omega)$.

An appropriate choice of the nominal model P_0 can reduce the size of the frequency dependent upper bound $\delta_{\mathrm{m}}(\omega)$ and therefore the size of the multiplicative uncertainty. Given Eq. 12, an appropriate choice for $P_0(\omega)$ is found by minimizing the worst case upper bound

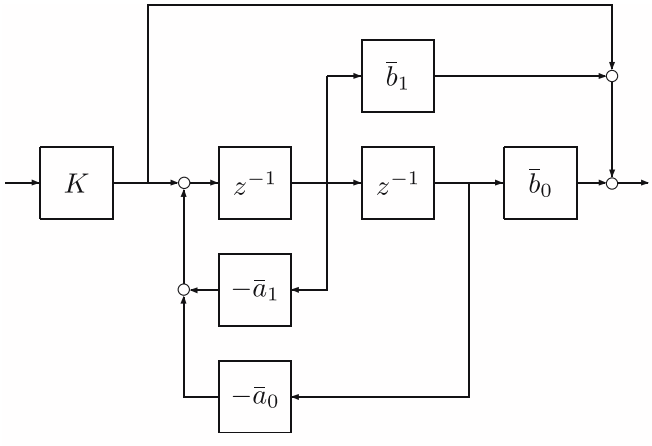

Fig. 5 Parametrization for characterization of damping and resonance frequency variations in discrete time model

$$P_o(\theta,\omega) = \min_{\theta} \max_{\omega\in\Omega} \delta_{\mathrm{m}}(\omega) \tag{13}$$

where θ indicates the free parameter of a parametrized nominal model $P_o(\theta)$. The nominal model $P_0(\theta)$ should have low complexity in order to provide a manageable control synthesis problem. Low complexity requirements on the nominal model rule out interpolation algorithms (Partington 1991; Pena and Snaizer 1995; Chen et al. 1996) to solve Eq. 13, as they tend to give fairly high order models.

A straightforward approach to the construction of a nominal model is to a two-step procedure in which an interpolation is followed by a curve fitting routine to provide the estimation of a low order model:

1. Compute an optimal nominal frequency response that minimizes the worst case frequency response upper bound in Eq. 12. This first step is a non-parametric characterization of the nominal behavior of the micro-actuator system in the form of a nominal frequency response.
2. Fit a nominal model $P_0(\theta)$ of specified low complexity to the optimal nominal frequency response data. This second step the actual nominal model P_0 of limited complexity for which the resulting frequency response upper bound in Eq. 12 can be evaluated.

These steps are outlined in the following.

4.2 Characterization of nominal frequency response

Let $F_k(\omega) \in \mathbb{C}$ represents the kth complex frequency response function (FRF) with $k = 1,\ldots,p$ and measured at a finite number of frequency points $\omega \in \Omega$, where Ω is a chosen frequency grid. Then the worst case upper bound for the multiplicative model error is given by

$$\delta_f(\omega) = \max_{k=1,\ldots,p} \left\| \frac{F_k(j\omega) - F_{\mathrm{nom}}(j\omega)}{F_{\mathrm{nom}}(j\omega)} \right\| \quad \omega \in \Omega \tag{14}$$

where $F_{\mathrm{nom}}(\omega)$ denotes the nominal FRF to be determined.

In order to find a nominal FRF $F_{\mathrm{nom}}(\omega) \in \mathbb{C}$ with the smallest multiplicative error $\delta_f(\omega)$, an optimization has to be solved for each $\omega \in \Omega$. By setting $F_{\mathrm{nom}}(\omega) = \alpha(\omega) + i\beta(\omega)$ the minimization of $\delta_f(\omega)$ with respect to $F_{\mathrm{nom}}(\omega)$ can be expressed as follows:

$$\delta_f(\omega) = \min_{\alpha(\omega),\beta(\omega)} \max_{k=1,\ldots,p} \left\| \frac{F_k(j\omega) - (\alpha(\omega) + i\beta(\omega))}{\alpha(\omega) + i\beta(\omega)} \right\| \tag{15}$$
$$\text{for } \omega \in \Omega.$$

The computation of $\alpha(\omega), \beta(\omega) \in \mathbb{R}$ in Eq. 15 is a convex optimization and guarantees a unique solution at every frequency $\omega \in \Omega$. The convexity of the problem for each frequency $\omega \in \Omega$ can be seen by the following formulation. Let $\alpha_k(\omega)$ and $\beta_k(\omega)$ be the real and imaginary part of the kth FRF $F_k(j\omega)$ at a frequency $\omega \in \Omega$. In order to obtain the minimum worst case upper bound, we can perform the following optimization for each $\omega \in \Omega$:

$$\min_{\alpha(\omega),\beta(\omega),r} r \quad \text{subjected to}$$
$$(\alpha(\omega) - \alpha_k(\omega))^2 + (\beta(\omega) - \beta_k(\omega))^2 \le (\alpha^2(\omega) + \beta^2(\omega))r$$
$$\text{for } k = 1,\ldots,p \tag{16}$$

where p is the number of FRF measurements. It should be noted that the computation of $F_{\mathrm{nom}}(\omega)$ via Eq. 16 at each $\omega \in \Omega$ does not resemble the geometric mean

$$\sum_{k=1}^{p} F_k(\omega)$$

as the geometric mean does not minimize the worst case multiplicative (or even additive) uncertainty bound $\delta_f(\omega)$ in Eq. 14.

As the multiplicative uncertainty description will be used to describe the manufacturing variations, the optimization (Eq. 16) is applied to the FRF measurements depicted in Fig. 3. For each frequency $\omega \in \Omega$ an optimal nominal FRF $F_{\mathrm{nom}}(\omega)$ is computed that minimizes the multiplicative error bound $\delta_f(\omega)$ given in Eq. 14. The result has been plotted in Fig. 6 and it can be observed that the nominal FRF is chosen such that the multiplicative error bound $\delta_f(\omega) < 1 \ \forall \ \omega \in \Omega$.

4.3 Estimation of a low order nominal model

The nominal FRF $F_{\mathrm{nom}}(\omega)$ is found by a frequency dependent worst case optimization of a multiplicative error bound. As $F_{\mathrm{nom}}(\omega)$, $\omega \in \Omega$ is still in the form of

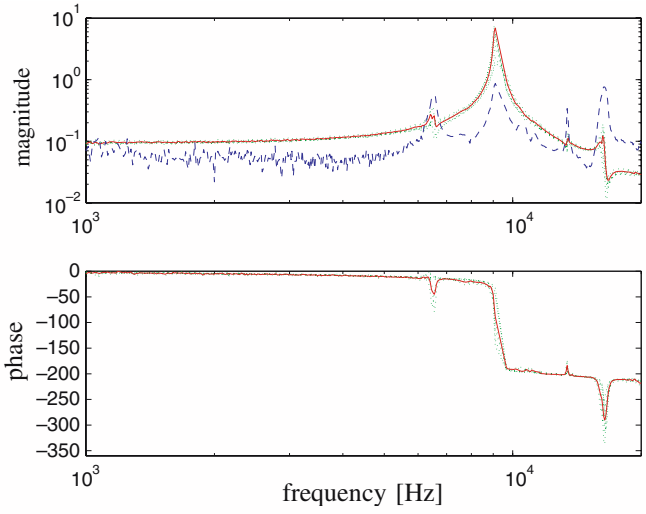

Fig. 6 Amplitude (*top*) and phase (*bottom*) Bode plot of the following frequency domain data: seven frequency response measurements $F_k(\omega)$, $k = 1,\ldots,7$ caused by manufacturing variations (*dotted*), the computed nominal frequency response $F_{\mathrm{nom}}(\omega)$ (solid) via Eq. 16, and the resulting minimum multiplicative error bound $\delta_f(\omega)$ (*dashed*) according to Eq. 14

frequency domain data points, a parametric nominal model of preferably low order is needed for controller synthesis.

For the discrete time servo control implementation in a HDD it is necessary to construct a discrete time (linear time invariant) model P_0 of limited complexity that approximates the nominal FRF $F_{\text{nom}}(\omega)$, $\omega \in \Omega$ as good as possible. To address the limited complexity, the nominal model P_0 to be determined is parameterized in a transfer function representation

$$P_0(z,\theta) = \frac{b_0 + b_1 z^{-1} + \cdots + b_n z^{-n}}{1 + a_1 z^{-1} + \cdots + a_n z^{-n}}, \tag{17}$$

where $z = e^{j\Delta T\,\omega}$ denotes the z-transform variable, ΔT the sampling time of the discrete tiem model and

$$\theta = [b_0, b_1, \ldots, b_n, a_1, \ldots, a_n]$$

denotes a real valued parameter of unknown coefficients in the transfer function representation given in Eq. 17. The order or complexity of the linear model can be specified with the integer value n.

The approximation of $F_{\text{nom}}(j\omega)$ by the model $P_0(z,\theta)$ is addressed by considering a curve fitting procedure. In the curve fitting procedure the following curve fitting error

$$E(\omega,\theta) = \frac{F_{\text{nom}}(\omega) - P_0(e^{j\omega},\theta)}{F_{\text{nom}}(\omega)} W(\omega), \quad \omega \in \Omega \tag{18}$$

is considered. In Eq. 18 a multiplicative error is being considered that is similar to Eq. 15. Additionally, a frequency dependent function $W(\omega)$ can be used to influence the curve fitting of the frequency response data.

The weighting function $W(\omega)$ plays an important role in finding a low order nominal model $P_0(\omega)$ by emphasizing the dynamics in the nominal FRF $F_{\text{nom}}(\omega)$ that are most relevant for control design. The choice of the proper weighting function $W(\omega)$ during estimation of a nominal model $P_0(\omega)$ can be used to take into account the control application of the model (Gaikwad and Rivera 1997; Van den Hof et al. 1997; Böling and Mäkilä 1998).

In order to motivate the choice of a weighting function $W(\omega)$, consider the problem of robust stability of a servo control loop in the presence of multiplicative modeling errors, similar as in Eq. 18 with $W(\omega) = 1$. For notation purposes, consider a scalar system P and servo controller C. In the presence of a multiplicative model error $\Delta_{\text{m}}(\omega) = [(P(\omega) - P_0(\omega))/P(\omega)]$, standard robust stability results (Zhou et al. 1996) indicate that

$$|\Delta_{\text{m}}(\omega)| \left| \frac{C(\omega)P(\omega)}{1 + C(\omega)P(\omega)} \right| < 1 \tag{19}$$

is a sufficient condition for stability robustness. Multiplicative modeling errors are weighted by the complementary sensitivity function $[CP/(1 + CP)]$ in the robust stability test (Eq. 19). Hence, minimization of the curve fitting error (Eq. 18) with a weighting function $W(\omega)$ that resembles $[C(\omega)P(\omega)/(1 + C(\omega)P(\omega))]$ will facilitate the robust stability test (Eq. 19). Such a frequency dependent weighting function $W(\omega)$, $\omega \in \Omega$ can be constructed by performing closed-loop experiments and measuring the complementary sensitivity function. Alternatively, the desired weighting function $W(\omega)$, $\omega \in \Omega$ can be realized by approximating the general shape of the complementary sensitivity function. In this way the weighting function $W(\omega)$ has a general shape that is chosen to be constant at low frequencies, a small increase at the cross-over frequency and a roll-off at high frequencies.

With the definition of the curve fitting error (Eq. 18), a parameter $\hat{\theta}$ is estimated by solving the following nonlinear weighted least squares minimization:

$$\hat{\theta} = \arg\min_{\theta} \sum_{\omega \in \Omega} E(\omega) E^*(\omega)$$

where * is used to denote the complex conjugate transpose. The estimation of the parameter $\hat{\theta}$ is solved by an iterative convex optimization and more results on the curve fitting procedure can be found in de Callafon et al. (1996). The curve fitting procedure is applied to the nominal FRF $F_{\text{nom}}(\omega)$ to estimate a nominal model P_0 of order $n = 6$ and a Bode plot of the model has been depicted in Fig. 7.

Along with the Bode plot of the nominal model P_0, the FRF measurements $F_k(\omega)$, $k = 1,\ldots,7$ given in Fig. 3 due to manufacturing variations, have been plotted. The resulting multiplicative error bound

$$\delta_{\text{m}}(\omega) = \max_{k=1,\ldots,p} \left\| \frac{F_k(j\omega) - P_0(e^{j\omega})}{P_0(e^{j\omega})} \right\| \quad \omega \in \Omega$$

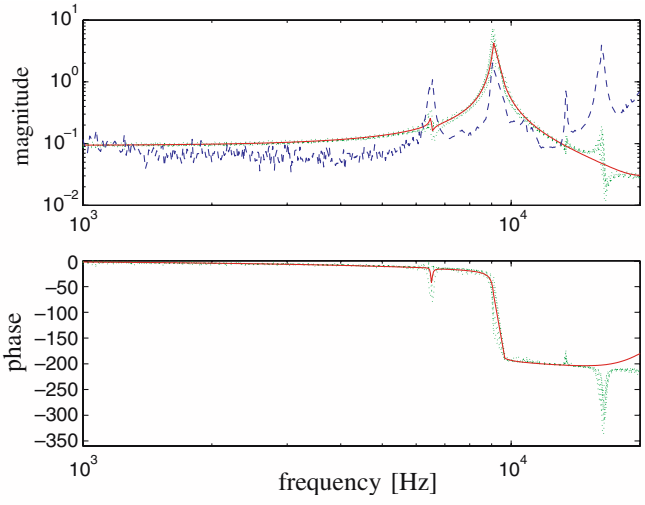

Fig. 7 Amplitude (*top*) and phase (*bottom*) Bode plot of the following frequency domain data: seven frequency response measurements $F_k(\omega)$, $k = 1,\ldots,7$ caused by manufacturing variations (*dotted*), the nominal sixth order discrete-time model $P_0(e^{j\omega})$ (*solid*) found via curve fitting $F_{\text{nom}}(\omega)$, and the resulting multiplicative error bound $\delta_m(\omega)$ (*dashed*) according to Eq. 12

has been plotted in the top portion of Fig. 7. With the definition of $\delta_f(\omega)$ in Eq. 14 it can be seen that $\delta_m(\omega) \geq \delta_f(\omega)$ in Fig. 6. This is due to the fact that a *low order* discrete time nominal model P_0 is estimated, resulting in a larger multiplicative error bound. Moreover, it can be observed that the multiplicative error bound $\delta_{\mathrm{m}}(\omega)$ is allowed to be larger at higher frequencies, which is motivated by the discussion on the weighting function $W(\omega)$ for robust stability analysis indicated above.

4.4 Unstructured uncertainty bound

To finalize the uncertainty model of the piezo-electric dual-stage actuator for manufacturing variations, a model W_{m} for the multiplicative model error has to be formulated. The model W_{m} is a parametric model that over bounds the unstructured multiplicative uncertainty bound. Next to the characterization of a nominal model P_0 in Eq. 6, a discrete time parametric model of the uncertainty weighting function W_{m} is needed for a discrete time robust controller synthesis. Similarly to the low order requirements on the nominal model, it is again advantageous to estimate a low order model for the uncertainty weighting function W_{m} to provide a manageable robust control design problem.

With the given estimated nominal model P_0, the resulting multiplicative model error bound

$$\delta_{\mathrm{m}}(\omega) = \max_{k=1,\ldots,p} \left\| \frac{F_k(j\omega) - P_0(\mathrm{e}^{j\omega})}{P_0(\mathrm{e}^{j\omega})} \right\| \quad \omega \in \Omega \tag{20}$$

needs to be over bounded by a stable and stably invertible discrete time transfer function $W_m(\mathrm{e}^{j\ \omega})$ such that

$$|W_{\mathrm{m}}(j\omega)| \geq \delta_{\mathrm{m}}(j\omega), \quad \forall \omega \in \Omega. \tag{21}$$

In this way, the multiplicative error bound $\delta_{\mathrm{m}}(\omega)$ is bounded from above by a *low order* weighting function W_{m}

$$\delta_{\mathrm{m}}(\omega) \leq |W_{\mathrm{m}}\Delta_{\mathrm{m}}|$$

where Δ_{m} is unknown, but bounded $||\Delta_{\mathrm{m}}||_\infty < 1$.

To address the limited complexity of the weighting function $W_{\mathrm{m}}(\omega)$, the weighting function W_{m} is parameterized in a transfer function representation based on a spectral factorization where

$$\begin{aligned} \tilde{W}_{\mathrm{m}}(\omega, \tilde{\theta}) &= W_{\mathrm{m}}(e^{j\omega}, \theta) W_m^*(\mathrm{e}^{j\omega}, \theta) \\ &= \frac{\beta_0 + \beta_1 2\cos(\omega) + \cdots + \beta_n 2\cos(n\omega)}{1 + \alpha_1 2\cos(\omega) + \cdots + \alpha_n 2\cos(n\omega)} \end{aligned} \tag{22}$$

in which * denotes the complex conjugate. In Eq. 22 the relation $z^k + z^{-k} = \mathrm{e}^{j\ k\ \omega} + \mathrm{e}^{-j\ k\ \omega} = 2\ \cos(k\ \omega)$, $k = 1,\ldots,n$ has been used to parametrize $\tilde{W}_{\mathrm{m}}(\omega)$. To simplify notations, the sampling time ΔT of the discrete time filter W_{m} is normalized to $\Delta T = 1$. The parameter $\tilde{\theta}$ to be estimated is given by

$$\tilde{\theta} = [\beta_0, \beta_1, \ldots, \beta_n, \alpha_1, \ldots, \alpha_n]$$

and the parameter θ in $W_{\mathrm{m}}(\mathrm{e}^{j\ \omega}, \theta)$ can be found by spectral factorization of $\tilde{W}_{\mathrm{m}}(\theta)$, provided $\tilde{W}_{\mathrm{m}}(\tilde{\theta}) > 0 \forall \omega$ (Åström 1970). Similarly as in Eq. 17, the order or complexity of the weighting function W_{m} can be specified with the integer value n.

The approximation and overbounding of the frequency dependent multiplicative upper bound $\delta_{\mathrm{m}}(\omega)$ by a discrete time parametric model $W_{\mathrm{m}}(\mathrm{e}^{j\ \omega})$ is addressed by formulating a spectral overbounding procedure similar as in Scheid et al. (1991) or Scheid and Bayard (1995). In the spectral overbounding procedure, the constrained min–max optimization

$$\begin{aligned} &\min_{\tilde{\theta}} \max_{\omega \in \Omega} \left| \left(\delta_m^2(\omega) - \tilde{W}_{\mathrm{m}}(\omega, \tilde{\theta}) \right) W(\omega) \right| \quad \text{subjected to} \\ &\tilde{W}_{\mathrm{m}}(\omega, \tilde{\theta}) \geq \delta_{\mathrm{m}}^2(\omega), \quad \omega \in \Omega \quad \tilde{W}_{\mathrm{m}}(\omega, \tilde{\theta}) > 0, \quad \forall \omega \end{aligned} \tag{23}$$

is solved via linear programming techniques. In Eq. 23 the maximum difference between the squared frequency dependent upper bound $\delta_{\mathrm{m}}^2(\omega)$ and the spectral model $\tilde{W}_{\mathrm{m}}(\omega)$ is minimized. Similar to Eq. 18, a frequency dependent weighting function $W(\omega)$ can be used to emphasize certain frequency areas in the squared frequency dependent upper bound $\delta_{\mathrm{m}}^2(\omega)$. The first constraint in Eq. 23 guarantees that $\tilde{W}_{\mathrm{m}}(\omega, \tilde{\theta})$ overbounds $\delta_{\mathrm{m}}^2(\omega)$, whereas the second constraint guarantees that $\tilde{W}_{\mathrm{m}}(\omega, \tilde{\theta})$ allows a spectral factorization $\tilde{W}_{\mathrm{m}}(\omega, \tilde{\theta}) = W_{\mathrm{m}}(\mathrm{e}^{j\omega}, \theta) W_{\mathrm{m}}^*(\mathrm{e}^{j\omega}, \theta)$ where $W_{\mathrm{m}}(\mathrm{e}^{j\ \omega}, \theta)$ is a stable and stably invertible discrete time transfer function. Choosing a weighting filter $W(\omega) = 1/\delta^2_{\{\mathrm{m}}(\omega)$ in Eq. 23 to emphasize a relative error during the constrained min–max optimization, the final result of the parametric multiplicative uncertainty overbounding has been plotted in Fig. 8.

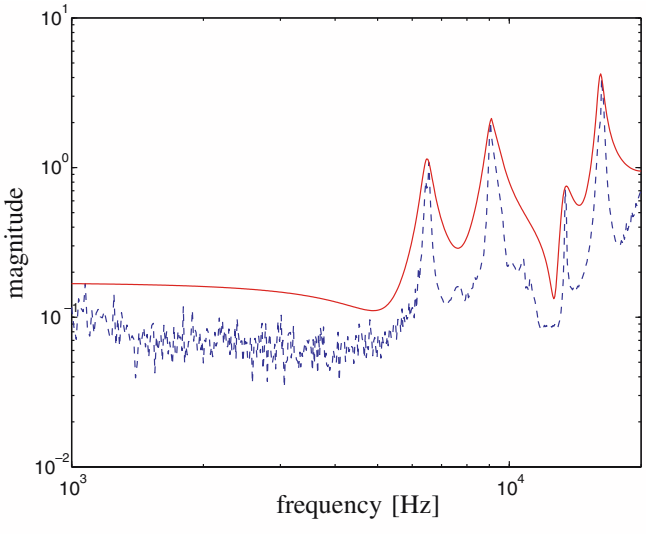

Fig. 8 Amplitude Bode plot of multiplicative error bound $\delta_{\mathrm{m}}(\omega)$ according to Eq. 20 (*dotted*) and computed stable and stably invertible 8th order model $W_{\mathrm{m}}(\mathrm{e}^{j\ \omega})$ (*solid*)

An amplitude Bode plot of the estimated stable and stably invertible weighting function $W_{\mathrm{m}}(\mathrm{e}^{j\,\omega})$ has been depicted in Fig. 8. The model $W_{\mathrm{m}}(\mathrm{e}^{j\,\omega})$ is an 8th order discrete time model that over bounds the unstructured multiplicative uncertainty bound $\delta_{\mathrm{m}}(\omega)$ for all $\omega \in \Omega$. It can be observed that the model $W_{\mathrm{m}}(\mathrm{e}^{j\,\omega})$ provides a tight overbound of $\delta_{\mathrm{m}}(\omega)$, especially at the peaks in the multiplicative uncertainty bound.

4.5 Structured parametric uncertainty bounds

In order to model the variations in the dynamic behavior of the HTI dual-stage actuator due to variations in Z-height, the structured uncertainty model $\mathscr{P}_z$ in Eq. 11 is used. In the structured uncertainty model $\mathscr{P}_z$, the Z-height variations are modeled by a varying torsion resonance/anti-resonance mode in the nominal model P_0 with nominal discrete time parameter values $b_{0,i}$, $a_{0,i}$ and a additive perturbation bounded by r_{b_i}, $r_{a,i}$ for $i=0,1$.

A nominal model P_0 is found by the curve fitting of the nominal FRF $F_{\mathrm{nom}}(\omega)$ and the result was depicted in Fig. 7. With this nominal model P_0, the nominal discrete time parameter values $b_{0,i}$, $a_{0,i}$ can be extracted by a decomposition of P_0 in

$$P_0(z) = \frac{z^2 + b_1 z + b_0}{z^2 + a_1 z + a_0} \bar{P}_0(z)$$

by isolating the estimated torsion resonance/anti-resonance mode around 6.5 kHz from the nominal model P_0. The variable transformation (Eq. 8) with $b_2 = a_2 = 1$ allows the nominal model P_0 to be rewritten into

$$P_0(z) = \left(1 + \frac{b_{0,1} z + b_{0,0}}{z^2 + a_{0,1} z + a_{0,0}}\right) K \bar{P}_0(z)$$

and the nominal values $b_{0,i}$, $a_{0,i}$, $i = 0,1$ for the structured uncertainty set $\mathscr{P}_z$ are extracted from the previously estimated nominal model P_0.

As the nominal model P_0 is constructed on FRF measurements involving a Z-height of 22 milli inches or 0.56 mm, the extreme Z-height situations of 0.30 and 0.82 mm can be used to characterize the additive parameter perturbations r_{b_i}, $r_{a,i}$, $i=0,1$ given in Eq. 10. The parameter perturbations are determined by curve fitting the FRF measurements $F_k(\omega)$, $k=1,2$ depicted in Fig. 4 for Z-height variations of 0.30 and 0.82 mm.

Similar to the nominal model $P_0(z)$, the models $P_k(z)$ found by curve fitting the FRF measurements $F_k(\omega)$ can be rewritten into

$$P_k(z) = \left(1 + \frac{b_{k,1} z + b_{k,0}}{z^2 + a_{k,1} z + a_{k,0}}\right) K \bar{P}_k(z)$$

where the estimated torsion resonance/anti-resonance mode around 6.5 kHz has been isolated. With this parametric information, the structured uncertainty set $\mathscr{P}_z$ can be completed by

$$r_{b,i} = \max_{k=1,2} \left| b_{k,i} - b_{0,i} \right|$$

$$r_{a,i} = \max_{k=1,2} \left| a_{k,i} - a_{0,i} \right|$$

for $i=0,1$. The results for the structured uncertainty estimation have been listed in Table 1, where both the nominal values and the additive parameter perturbations have been listed.

It can be observed from Table 1 that all parameters have additive perturbations smaller than their nominal value. This avoids a sign change of the parameters in the structured uncertainty model $\mathscr{P}_z$ in Eq. 11. As mentioned before, the structural variations due to Z-height variations are much larger than typically observed in a suspension mounted in a HDD. This is due to the excessive variations from 0.30 to 0.82 mm for the Z-height variations in our experiments. These variations were only used to demonstrate the effectiveness of capturing possible structural variations in the torsion mode of the suspension.

To indicate the effect for the structured uncertainty model, consider the Bode plot given in Fig. 9. In Fig. 9 the structural change in the torsion mode can be observed in the form of a change in damping of the resonance/anti-resonance mode, as observed in the FRF measurements depicted in Fig. 4. It should be stressed that with the proposed structured uncertainty model $\mathscr{P}_z$, only a structural change in the torsion mode of the piezo-electric milli-actuator due to Z-height variations has been modeled. Additional variations of resonance modes can be incorporated in the structured uncertainty model, at the price of additional complexity of the uncertainty model. As the torsion mode is considered to be of great importance in robust control design, the structured uncertainty model only takes into account the variations in this first resonance mode of the piezo-electric micro-actuator.

Summarizing, the product variabilities observed in experimental data obtained from several HTI Magnum 5E piezoelectric dual-stage suspension can be modeled by a nominal model P_0 with a unstructured multiplicative uncertainty bounded by $W_{\mathrm{m}}(\omega)$. The Z-height variations are modeled by a varying resonance/anti-resonance mode in the nominal model P_0 with nominal discrete time parameter values $b_{0,i}$, $a_{0,i}$ and an additive perturbation of the parameters bounded by r_{b_i}, $r_{a,i}$ for $i=0,1$. Both product variabilities can be combined in a single LFT based uncertainty model $\mathscr{P}$ similarly to Eq. 5

Table 1 Numerical values of the structured uncertainty model $\mathscr{P}_z$ in (9)

Nominal values		Additive perturbation	
$b_{0,0}$	-3.93×10^{-3}	$r_{b,0}$	3.71×10^{-3}
$b_{0,1}$	4.29×10^{-2}	$r_{b,1}$	3.34×10^{-2}
$a_{0,0}$	0.98	$r_{a,0}$	1.69×10^{-3}
$a_{0,1}$	-1.075	$r_{a,1}$	3.27×10^{-2}

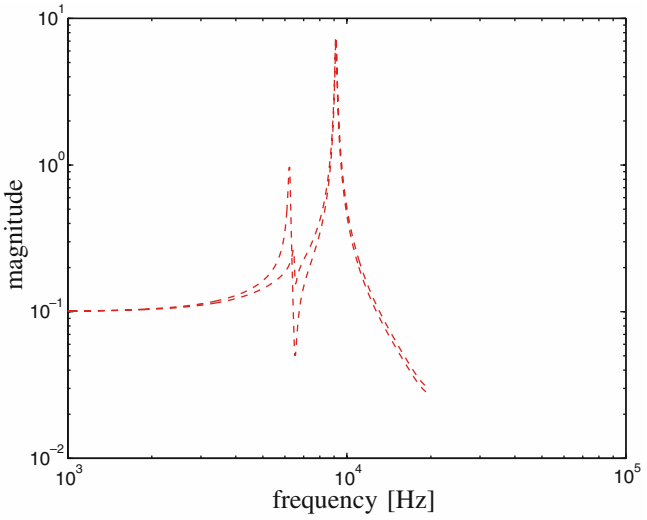

Fig. 9 Amplitude Bode plot of structured uncertainty model $\mathscr{P}_z$ (Eq. 11) with maximum and minimum structured perturbation

where the uncertainty Δ has been normalized and structured in a diagonal form $\Delta = \text{diag}\ (\delta_{b,1},\delta_{b,0},\delta_{a,1},\delta_{a,0},\Delta_m)$ where $|\delta_{b,i}| < 1$, $i = 0,1$, $|\delta_{a,i}| < 1$, $i = 0,1$ and $\| \Delta_m \|_\infty < 1$. Since the uncertainty model is constructed and validated on experimental data, it forms an excellent basis for the robust servo control design of the piezoelectric dual-stage suspension system.

5 Conclusions

In this paper a systematic modeling procedure is presented for obtaining a nominal model and an uncertainty bound based on experimental frequency response data. The procedure is applied and illustrated on a micro-electromechanical system that consists of a HDD piezoelectric dual-stage suspension manufactured by HTI. This research is motivated by the design of high performance and robust dual-stage suspensions controllers for hard disk drives. Under product variations and changing of operating conditions of the micro-electromechanical system, uncertainty modeling is necessary to guarantee robustness of the feedback controllers. In addition, small and non-conservative uncertainty descriptions are needed to attain high performance servo requirements in high track density recording.

For this application, product variabilities are separated in structured and unstructured uncertainties and both are characterized via efficient frequency domain based optimization techniques. For characterization of the unstructed uncertainy, the modeling procedure consists of two steps, where first an optimal nominal frequency response is computed that minimizes the worst case multiplicative frequency response upper bound. In the second step, a low complexity nominal model for the nominal frequency response and a weighting function that overbounds the multiplicative uncertainty are obtained via frequency response curve fitting. The nominal model is found via an iterative least-squares solution, while the weighting function is obtained via a linear programming problem, both of which can be solved relatively easily. For the characterization of the structured uncertainty, models are estimated that capture specific perturbation in one of the resonance modes of the micro-electromechanical system. Using a framework based on linear fractional transformation, parameter perturbations are written in an explicit form and the parametric uncertainty model is combined with the unstructured multiplicative uncertainty to complete the uncertainty modeling of the micro-electromechanical system.

References

Åström KJ (1970) Introduction to stochastic control theory. Academic, New York

Böling JM, Mäkilä PM (1998) On control relevant criteria in H_∞ identification. IEEE Trans Autom Control 43(5):694–700

de Callafon RA, Roover D, Van den Hof PMJ (1996) Multivariable least squares frequency domain identification using polynomial matrix fraction descriptions. In: Proceedings of the 35th IEEE conference on decision and control, Kobe, Japan, pp 2030–2035

de Callafon RA, Harper DHF, Skelton RE, Talke FE (1999) Experimental modeling and feedback control of a piezo-based milliactuator. J Inform Storage Process Syst 1(3):217–224

Chen J, Farell JA, Nett CN, Zhou K (1996) H_∞ identification of multivariable systems by tangential interpolation methods. IEEE Trans Autom Control 41(12):1822–1828

Fan LS, Ottesen HH, Reiley TC, Wood RW (1995) Magnetic recording head positioning at very high track densities using a microaactuator-based, two-stage servo system. IEEE Trans Indus Electron 42(3):222–223

Gaikwad SV, Rivera DE (1997) Multivariable frequency-response curve fitting with application to control-relevant parameter estimation. Automatica 33(6):1169–1174

Hernandez D, Park S, Horowitz R, Packard A (1999) Dual-stage track-following servo design for hard disk drives. In: Proceedings of the American control conference, San Diego, pp 4116–4121

Li Y, Horowitz R (2002) Design and testing of track-following controllers for dual-stage servo systems with pzt actuated suspensions. Microsyst Technol 8:194–205

Li Y, Horowitz R, Evans R (2003) Vibration control of a pzt actuated suspension dual-stage servo system using a pzt sensor. IEEE Trans Magn 39:932–937

Ljung L (1999) System identification: theory for the user, 2nd edn. Prentice-Hall, Englewood Cliffs

Partington JR (1991) Robust identification and interpolation in H_∞. Int J Control 54:1281–1290

Pena S, Snaizer RS (1995) Robust identification with mixed time/frequency experiments: consistency and interpolation algorithms. In: Proceedings of the 34th IEEE conference on decision and control, New Orleans, pp 234–236

Rotunno M, de Callafon RA (2000) Fixed order H_∞ control design for dual-stage hard disk drives. In: Proceedings of the 39th IEEE conference on decision and control, vol 4, Sydney, Australia, pp 3118–3119

Scheid RE, Bayard DS (1995) A globally convergent minimax solution for spectral overbounding and factorization. IEEE Trans Autom Control 40(4):712–716

Scheid RE, Bayard DS, Yam Y (1991) A linear programming approach to characterizing norm bounded uncertainty from experimental data. In: Proceedings of the American control conference, Boston, pp 1956–1958

Skogestad S, Postlethwaite I (1996) Multivariable feedback control. Wiley, Chichester

Teerjuis AP, Cools SJM, de Callafon RA (2003) Reduction of flow induced suspension vibrations in a hard disk drive by dual-stage suspension control. IEEE Trans Magn 39(5):2237–2239

Van den Hof PMJ, van Donkelaar ET, Dötsch HGM, de Callafon RA (1997) Control-relevant uncertainty modelling directed towards performance robustness. In: Proceedings of the 13th IFAC world congress, San Francisco, pp 103–108

Zhou K, Doyle JC (1998) Essentials of robust control. Prentice-Hall, Upper Saddle River

Zhou K, Doyle JC, Glover K (1996) Robust and optimal control. Prentice-Hall, Upper Saddle River